frontiers | Frontiers in Environmental Science

TYPE Original Research
PUBLISHED 09 May 2023
DOI 10.3389/fenvs.2023.1142941

OPEN ACCESS

EDITED BY
Ying Li,
Chinese Academy of Sciences (CAS), China

REVIEWED BY
Yimeng Song,
Yale University, United States
Masao Gen,
Tohoku University, Japan
Yangxi Chu,
Chinese Research Academy of Environmental Sciences, China

*CORRESPONDENCE
Mijung Song,
mijung.song@jbnu.ac.kr

RECEIVED 12 January 2023
ACCEPTED 24 April 2023
PUBLISHED 09 May 2023

CITATION
Gaikwad S, Kim D, Jeong R, Lee JY, Lee K, Ahn J, Jang K-S, Kim C and Song M (2023), Morphology and phase state of $PM_{2.5}$ in urban and coastal-rural areas during summer.
Front. Environ. Sci. 11:1142941.
doi: 10.3389/fenvs.2023.1142941

Morphology and phase state of $PM_{2.5}$ in urban and coastal-rural areas during summer

Sanjit Gaikwad[1], Daeun Kim[1], Rani Jeong[1], Ji Yi Lee[2], Kwangyul Lee[3], Junyoung Ahn[4], Kyoung-Soon Jang[5], Changhyuk Kim[6] and Mijung Song[1,7]*

[1]Department of Environment and Energy, Jeonbuk National University, Jeonju-si, Republic of Korea, [2]Department of Environmental Science and Engineering, Ewha Womans University, Seoul, Republic of Korea, [3]Division of Climate and Air Quality Research, National Institute of Environmental Research, Chungcheong Region Air Quality Research Center, Seosan, Republic of Korea, [4]Department of Atmospheric Environment Research, National Institute of Environmental Research, Seoul, Republic of Korea, [5]Bio-Chemical Analysis Team, Korea Basic Science Institute, Cheongju, Republic of Korea, [6]School of Civil and Environmental Engineering, Pusan National University, Busan, Republic of Korea, [7]Department of Earth and Environmental Sciences, Jeonbuk National University, Jeonju-si, Republic of Korea

The morphology and phase state are critical physical properties of aerosol particles. However, studies related to the analysis of these properties primarily focus on laboratory experiments, and studies on real aerosol particles are limited. Herein, fine particulate matter ($PM_{2.5}$) filter samples were obtained to investigate and compare the morphology and phase state of ambient aerosol particles in South Korea. The $PM_{2.5}$ samples were collected in the summer of June 2021 from two different environments: Seoul (urban) and Seosan (coastal-rural). Optical microscopy was combined with the poke-and-flow technique to determine the morphology and phase state of the $PM_{2.5}$ as a function of relative humidity (RH) at 293 $\pm$ 1 K. At both sites, the $PM_{2.5}$ droplets, which were extracted in purified water, showed a multiphase nature that was dependent on the RH and chemical composition. Based on the results and ambient average RH in Seoul, most of the $PM_{2.5}$ was observed in a liquid state on polluted days under an inorganic-dominant condition, but in a semisolid state on clean days under an organic carbon-rich condition. In Seosan, the $PM_{2.5}$ predominantly existed in a liquid state, due to the high RH caused by proximity to the Yellow Sea. Our study provides fundamental physical properties of $PM_{2.5}$ for both urban and coastal-rural environments. The results have strong applications for atmospheric chemistry and predicting particle size distributions.

KEYWORDS

liquid, semisolid, solid, air pollution, aersol

1 Introduction

In Asia, rapid industrialization and infrastructure developments have resulted in environmental issues associated with an increase in air pollution and a decrease in air quality (Masson-Delmotte et al., 2021). Among the various atmospheric pollutants, fine particulate matter ($PM_{2.5}$) significantly affects climate change and human health (Song Y. et al., 2019; Bhattarai et al., 2020; Masson-Delmotte et al., 2021). These effects are influenced by the physicochemical properties of $PM_{2.5}$, including chemical composition, size, phase state, and morphology (Seinfeld and Pandis. 2016). Field studies have reported that $PM_{2.5}$ is

predominately comprised of a mixture of thousands of organic molecules and some inorganic substances (Jimenez et al., 2009; Zhang et al., 2011; Kim et al., 2022).

$PM_{2.5}$ can undergo phase transitions in the atmosphere, resulting in different morphologies and phase states. Depending on the relative humidity (RH), temperature, and particle chemical composition, $PM_{2.5}$ morphology can shift between being homogeneous, core–shell, or partially engulfed (Reid et al., 2011; Song et al., 2013). Studies using atmospherically relevant particles have shown that aerosol particles often exhibit a phase-separated morphology when the oxygen-to-carbon ratio (O: C) of their organic materials is less than 0.8 (Bertram et al., 2011; Krieger et al., 2012; Song et al., 2012; Zuend and Seinfeld. 2012). These different morphologies can affect the heterogeneous chemical reaction rate, water uptake, and gas-to-particle partitioning (Zuend and Seinfeld. 2012; Lam et al., 2021; Mikhailov et al., 2021).

$PM_{2.5}$ can exist in a liquid, semisolid, or solid phase state in the atmosphere, and the phase state is vital for predicting the size distribution, mass concentration, heterogeneous reactivity, and ice nucleation efficiency of its particles (Shiraiwa et al., 2013; Kim et al., 2019; Knopf et al., 2018; Li et al., 2018; Zaveri et al., 2018). The phase state of $PM_{2.5}$ can be determined by the range of viscosity, where liquid (viscosity < 10^2 Pa s), semisolid (viscosity of 10^2–10^{12} Pa s), and solid (viscosity > 10^{12} Pa s) (Koop et al., 2011). Various laboratory studies have shown that the RH, water affinity, and chemical composition of aerosol particles significantly impact their phase states (Koop et al., 2011; Grayson et al., 2016; Rothfuss and Petters. 2017; Song M. et al., 2019; Champion et al., 2019; Petters et al., 2019; Song et al., 2021; Ham et al., 2019; Jeong et al., 2022). However, comparatively few field studies have observed the phase states of real-world aerosol particles (Bateman et al., 2016; Liu et al., 2021b; Cheng et al., 2021; Song et al., 2022). More data on the morphologies and phase states of real-world aerosol particles are required to accurately describe the impact of aerosols on atmospheric chemistry and the climate.

To achieve this, $PM_{2.5}$ was simultaneously collected at two different sites in South Korea in June 2021 including Seoul (urban) and Seosan (coastal-rural). Seoul is a highly populated urban area and one of the world's megacities, whereas Seosan is a coastal-rural area surrounded by an agricultural complex, the Yellow Sea, and coal power plants. Morphologies and phase states of $PM_{2.5}$ droplets were observed at 293 ± 1 K upon dehydration, using optical microscopy and a poke-and-flow technique. The results of these two methods were combined with ambient RH conditions to estimate and compare the phase states of $PM_{2.5}$ in these urban and coastal-rural areas during summer.

2 Materials and methods

2.1 Measurement sites

$PM_{2.5}$ filter samples were simultaneously collected in Seoul (37.61°N, 126.93°E) and Seosan (36.78°N, 126.49°E) in South Korea during June 1–30, 2021 (Supplementary Figure S1). Seoul is a megacity with heavy traffic and dense residential areas (Kim et al., 2022). The sampling site in Seoul was operated by the National Institute of Environmental Research in Bulgwang-dong, Eunpyeong-gu. Seosan is a coastal-rural area surrounded by agricultural clusters, ~15 km from the Yellow Sea, and ~26 km from petrochemical complexes. This site has one of the highest annual $PM_{2.5}$ levels in Korea, even though it is a rural area (Ju et al., 2020). The Seosan measurement site was operated by the National Institute of Environmental Research in Suseok-dong, Seosan-si, Chungcheongnam-do.

2.2 Collection and generation of $PM_{2.5}$

$PM_{2.5}$ was collected on quartz filters (8 × 10 inches, Pall Co., United States) every 23 h (from 10:00 a.m. to 09:00 a.m., local time) using high-volume air samplers at a flow rate of ~1000 L/m (HV-1000R, SIBATA, Japan). The samples were immediately stored in a freezer at ~255 K after collection. We focused on samples with high $PM_{2.5}$ concentrations at least one of the two sites, i.e., a daily mean concentration ≥35 μg/m^3, which is the standard daily level of $PM_{2.5}$ in Korea (Ministry of Environment, 2021). Based on this, six cases (Cases 1–6) were selected from both sites (yellow shaded regions in Supplementary Figure S2), which included high $PM_{2.5}$ episodes. The samples in Cases 1–6 that were considered unsuitable for analysis were excluded, such as the sample collected in Seosan on 28 June 2021, owing to the considerably low surface tension of the $PM_{2.5}$ droplets on the substrate. In total, 17 filter samples (nine from Seoul and eight from Seosan) were investigated for phase states. Table 1 provides information on the daily mean concentrations, chemical compositions (Supplementary Section S1), O:C (Supplementary Section S2), and aerosol liquid water content (Supplementary Section S3) of $PM_{2.5}$ for Cases 1–6 in Seoul and Seosan. An overview of the measurements at the two different sites is provided in Supplementary Section S4. The filter samples for Cases 1–6 were extracted as water-soluble organic and inorganic compounds in deionized water (18.2 MΩ cm, Merck Milli-Q®, Millipore, United States) for morphology and phase experiments within 3 months after collection. Previous studies showed that water-soluble organic and inorganic species were comprised of more than ~70% in $PM_{2.5}$ (Huang et al., 2012; Liu et al., 2021a). A nebulizer (MEINHARD®, United States) was used to nebulize the extracted $PM_{2.5}$ droplets onto a hydrophobic substrate for morphology observation (Section 2.3) and poke-and-flow experiments (Section 2.4).

2.3 Optical microscopy for $PM_{2.5}$ droplets

A flow-cell was used to perform temperature- and RH-controlled measurements for $PM_{2.5}$ droplets on a hydrophobic substrate (Song et al., 2012; Jeong et al., 2022). The $PM_{2.5}$ droplets were equilibrated at ~100% RH and 293 ± 1 K for ~20 min at the start of the experiment. The RH was then lowered at a rate of 0.5% RH/min. Morphological analysis was carried out using an optical microscope; detailed procedures and methods are described in previous reports (Gaikwad et al., 2022; Song et al., 2022). An optical microscope (BX4 × 3, ×40 objective; Olympus, Japan) was used to monitor and capture morphology changes at 10 s intervals during the dehydration process, using a camera with a charge-coupled device (CCD) (DigiRetina 16, Tucsen,

TABLE 1 A summary of the average daily mass concentration, chemical composition, oxygen-to-carbon ratio (O:C), and aerosol liquid water content (ALWC) of $PM_{2.5}$, and ambient relative humidity (RH) based on filter sampling intervals in seoul and seosan for Case 1–6 in 2021. Phase state of the bulk of $PM_{2.5}$ at mean ambient RH is also included.

Date	$PM_{2.5}$	NH_4^+	NO_3^-	SO_4^{2-}	OC	EC	O:C	ALWC	Ambient RH	Phase state
	(μg/m^3)	(μg/m^3)	(μg/m^3)	(μg/m^3)	(μg/m^3)	(μg/m^3)		(μg/m^3)	(%)	At mean RH
Seoul										
06.05	45.9	7.9	12.4	10.0	5.1	1.2	0.45	41.2	71.1	Liquid
06.09	33.0	2.2	3.9	3.3	8.1	1.8	0.49	6.0	56.7	Semisolid
06.12	15.5	0.9	1.0	2.0	3.9	0.7	0.49	3.9	72.0	Semisolid
06.13	24.7	2.4	3.0	4.1	5.2	1.0	0.45	10.0	72.0	Semisolid
06.14	42.6	6.0	12.7	5.4	8.0	1.5	0.45	21.8	68.1	Semisolid
06.19	40.3	7.1	11.2	8.9	4.8	0.7	0.44	31.5	71.0	Semisolid
06.20	51.2	9.9	17.1	11.1	5.0	1.0	0.50	61.2	74.4	Liquid
06.24	37.8	5.9	8.9	7.8	4.3	0.8	0.46	24.5	70.3	Semisolid
06.28	15.9	1.6	1.0	4.0	3.2	0.6	0.51	7.5	77.1	Semisolid
Mean	34.1	4.9	7.9	6.3	5.3	1.0	0.47	23.1	70.3	
Seosan										
06.05	45.7	6.8	11.7	7.5	5.9	0.8	0.47	94.4	84.0	Liquid
06.09	31.5	3.7	3.8	5.1	8.2	1.0	0.46	23.2	66.9	Semisolid
06.12	24.3	4.0	6.5	4.4	4.8	0.6	0.46	44.2	79.8	Liquid
06.13	20.5	3.8	4.1	5.4	2.6	0.4	0.46	130.9	85.6	Liquid
06.14	24.3	4.5	6.1	5.4	3.6	0.6	0.47	28.1	82.3	Liquid
06.19	33.9	6.4	9.9	7.0	3.2	0.4	0.47	187.9	83.3	Liquid
06.20	48.7	9.1	15.3	9.2	5.2	0.8	0.51	152.1	81.3	Liquid
06.24	26.0	4.2	6.8	4.5	4.0	0.5	0.47	132.9	82.3	Liquid
Mean	31.9	5.3	8.0	6.1	4.7	0.7	0.47	105.4	80.7	

China). The RH in the flow-cell was calibrated at 293 ± 1 K by measuring the deliquescence RH of K_2CO_3 (at 44% RH) and NaCl (at 76% RH) (Winston and Bates. 1960), resulting in RH uncertainty of ±1.5%. The RH in the flow-cell was adjusted by the ratio of dry N_2 gas to saturated H_2O gas (total flow rate: 500 sccm). The temperature range of the experiment (293 ± 1 K) was similar to the actual mean temperature in Seoul (297 ± 3 K) and Seosan (295 ± 3 K).

2.4 Poke-and-flow technique for $PM_{2.5}$ droplets

A poke-and-flow technique was adopted to analyze the $PM_{2.5}$ phase state as semisolid or solid, hereafter referred to as (semi) solid as described by Renbaum-Wolff et al. (2013); Song M. et al. (2019). The procedure was detailed in previous studies (Renbaum-Wolff et al., 2013; Gaikwad et al., 2022). The $PM_{2.5}$ droplets were conditioned at ~ 100% RH. Subsequently, the RH was decreased to ~40% at a rate of ~1% RH/min, and the RH was then adjusted from approximately 40% to 0% at ~ 10% decrements. At a given RH, the droplets were conditioned for ~2 h before being poked. A sharp needle (Jung Rim Medical Industrial, South Korea) was used to poke the droplets at each decrement to determine the RH at which the particles cracked. Subsequently, the geometry was observed for ~3 h to observe the occurrence of fluid flow. Based on previous studies using the poke-and-flow technique, when no flow was observed, the viscosity was determined to be > ~1 × 10^8 Pa·s (Song et al., 2015; Grayson et al., 2016). However, this technique did not allow for measurements in the semisolid viscosity range of 10^2–10^8 Pa·s because the $PM_{2.5}$ was supersaturated with inorganic substances such as ammonium sulfate and ammonium nitrate upon dehydration. The $PM_{2.5}$ droplets were observed with an optical microscope (CKX5 × 3, ×40 objective; Olympus, Japan) before, during, and after being poked; the process was captured using a CCD camera (C11440-42U30, Hamamatsu, Japan). A temperature of ~293 ± 1 K was maintained during the experiments, which reflected the ambient temperature range recorded at the two sampling sites.

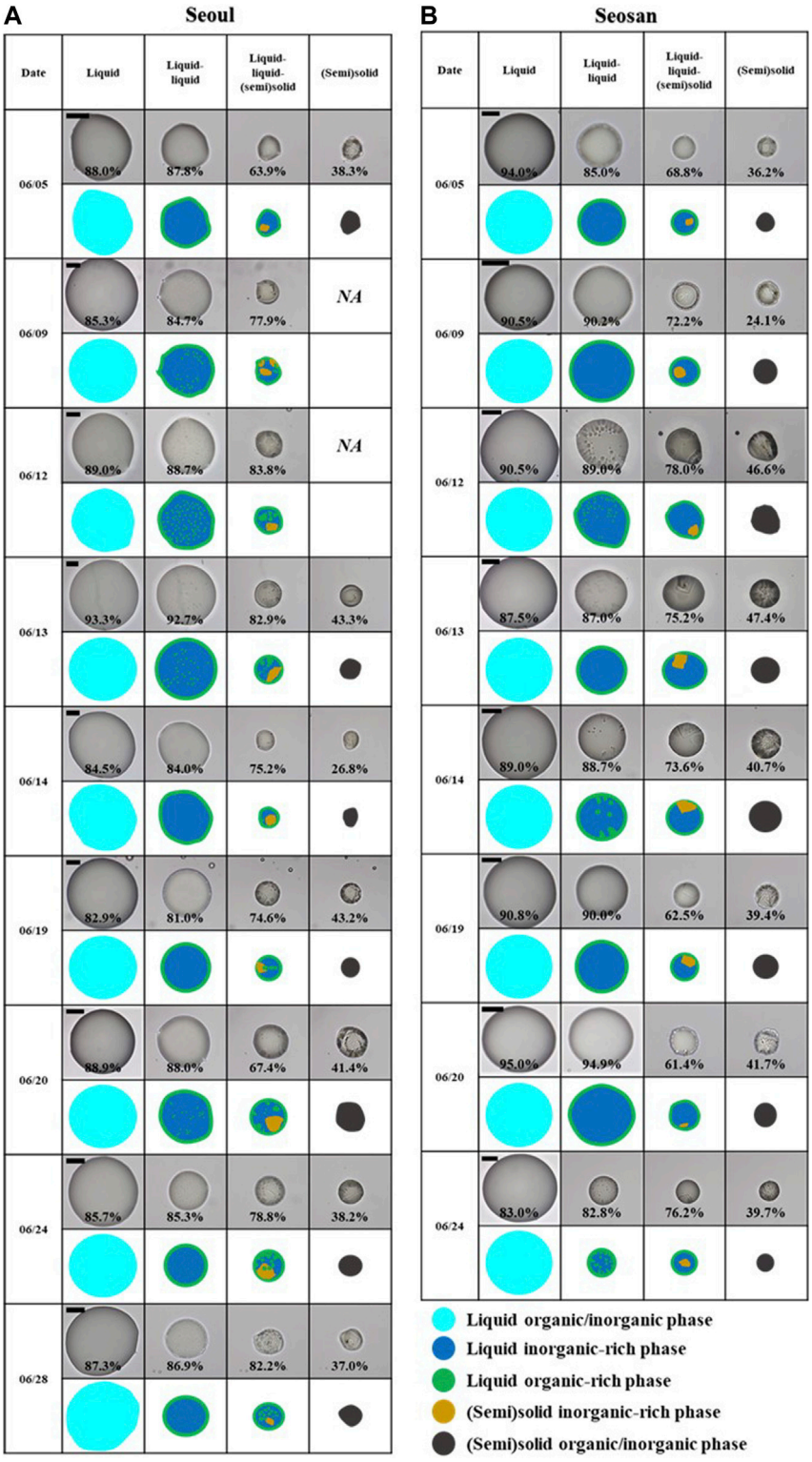

FIGURE 1
Optical images of the morphology changes of $PM_{2.5}$ droplets at 293 ± 1 K with decreasing relative humidity (RH) for **(A)** seoul and **(B)** seosan. *"NA"* denotes the droplet morphology that was not observed optically. Cartoons are provided to assist in the interpretation of the observed morphologies. Cyan: liquid organic/inorganic phase; blue: liquid inorganic-rich phase; green: liquid organic-rich phase; dark yellow: (semi) solid inorganic-rich; and dark grey: (semi) solid organic/inorganic phase. The scale bar in the optical images denotes 20 μm.

3 Results and discussion

3.1 Morphology of $PM_{2.5}$ droplets

$PM_{2.5}$ was collected in the summer of 2021 in the urban and coastal-rural environments of Seoul and Seosan, respectively, including high $PM_{2.5}$ episodes. The samples for each site were labeled as Cases 1–6 (per site), and the morphology of the $PM_{2.5}$ was studied at a temperature of 293 ± 1 K. Figures 1A, B show the changes in $PM_{2.5}$ morphology during the dehydration process in Seoul and Seosan, respectively, for each date. All components were dissolved in the droplets at an RH of ~100–90%, exhibiting a single liquid state (as shown in the second column in Figures 1A, B). The evaporation of water from the droplets caused the size to decrease with decreasing RH. At an average of ~87–89% RH, all $PM_{2.5}$ droplets showed liquid-liquid phase separation (LLPS) (third column in Figures 1A, B). This LLPS has been observed in numerous laboratory studies and modeling work, and commonly occurs when the O: C ratio of organic materials in the presence of inorganic salts is below 0.8 (Bertram et al., 2011; Song et al., 2012; Zuend and Seinfeld. 2012). LLPS has also been observed in ambient aerosol particles from different environments, within a specified range of O: C ratios (Pöhlker et al., 2012; You et al., 2012; Gaikwad et al., 2022; Song et al., 2022). In this study, the average O: C of the $PM_{2.5}$ droplets was ~0.47 at both sites (Table 1), which is within the appearance range for LLPS.

The equilibrium morphology of liquid-liquid-phase separated droplets (i.e., core–shell or partially engulfed) can be determined by the surface and interfacial tensions and spreading coefficients of the two phases (Kwamena et al., 2010; Song et al., 2013). In the droplets from both sites, a core-shell morphology was observed on a hydrophobic substrate. Previous studies have shown that liquid-liquid-phase-separated particles with a core-shell morphology predominantly consist of organic and inorganic species on their outer and inner phases, respectively (Ciobanu et al., 2009; Reid et al., 2011; Song et al., 2013). This can be explained by the fact that organic compounds possess a lower surface tension than inorganic salts (Ciobanu et al., 2009).

With a further decrease in RH, crystals abruptly appeared inside the $PM_{2.5}$ droplets (fourth column of Figures 1A, B), leading to a three-phase coexistence of a liquid-liquid-(semi) solid state, occurring at an average RH range of ~76–27% for Seoul and ~71–33% for Seosan. The crystals may be solid organic materials or inorganic substances such as ammonium sulfite and ammonium nitrate. This morphology has not yet been observed in laboratory-made aerosol particles. However, recently, the coexistence of the three phases consisting of liquid-liquid-(semi) solid has been discovered in the $PM_{2.5}$ of different environments (Gaikwad et al., 2022; Song et al., 2022). This suggests that atmospheric aerosol particles could display more complicated and multi-phase morphologies than their laboratory counterparts. This finding can be used to predict more accurate results for heterogeneous reactions and in atmospheric chemistry (Riemer et al., 2019). As shown in Figure 1 (last column), a further decrease in RH led to the efflorescence of a large portion of the inorganic fractions.

3.2 Phase states of $PM_{2.5}$ as a function of RH

To determine a (semi) solid state of the $PM_{2.5}$, a poke-and-flow experiment was performed at ~293 ± 1 K. All $PM_{2.5}$ droplets cracked when poked by a needle at average RHs of ~27% and ~33% for particles collected in Seoul and Seosan, respectively (Figure 2). After cracking, no flow was observed for a period of ~3 h, indicating a viscosity lower limit of ~10^8 Pa·s (Song et al., 2015; Grayson et al., 2016), which corresponds to a (semi) solid state (Koop et al., 2011).

From the result of the optical microscopy and poke-and-flow experiments, the phase states of the "bulk" of $PM_{2.5}$ were determined as a function of RH at a temperature of ~293 ± 1 K. The bulk of the $PM_{2.5}$ was characterized as "liquid" for single liquid and liquid-liquid phase separated particles, "semisolid" for liquid-liquid-(semi) solid particles (although not all phases in the particles were necessarily semisolid), and "(semi) solid" for semisolid or solid particles (Song et al., 2022). Based on this characterization, Figure 3A presents the phase states of $PM_{2.5}$ in Cases 1–6 from the two study sites (dates are shown for increasing daily $PM_{2.5}$ concentrations). The bulk of the $PM_{2.5}$ from Seoul exhibited a liquid state at mean RHs > ~87%, semisolid state at ~27% < mean RHs < ~76%, and (semi) solid state at mean RHs < ~27%. In Seosan, the bulk of the $PM_{2.5}$ was a liquid state at mean RHs > ~89%, semisolid state at ~33% < mean RHs < ~71%, and (semi) solid state at mean RHs < ~33%. The average RH range of the liquid state was similar in the two sites, while the RH range of the (semi) solid state was slightly higher in Seosan (~33%) than that in Seoul (~27%).

Interestingly, a clear difference in the RH boundary of semisolid and (semi) solid state was observed in Seoul. It was ~38% RH on polluted days ($PM_{2.5} \geq 35$ μg/m^3), but the RH value was dropped down to ~13% on clean days ($PM_{2.5} < 35$ μg/m^3) as shown in Figure 3A. This is most likely due to the different chemical compositions of Seoul $PM_{2.5}$ on polluted and clean days; Figure 3B and S3a illustrate the abundance of major chemical compositions of $PM_{2.5}$ in Seoul for polluted *versus* clean days, including organic carbon (OC), elemental carbon (EC), and inorganic substances (sulfate, nitrate, and ammonium). A distinct difference in $PM_{2.5}$ chemical compositions was monitored in Seoul that inorganic fraction increased to ~81% on polluted days while it was decreased to ~55% with enhancement of organic fraction on clean days. Recent laboratory studies have shown the effect of inorganic salts on viscosity and phase state in aerosol particles (Richards et al., 2020; Jeong et al., 2022). Jeong et al. (2022) showed that the viscosity of inorganic-rich particles (i.e., ammonium sulfate) was approximately 8 orders of magnitude higher than that of organic-rich particles at low RH levels close to their efflorescence RH. In the current study, the effect of inorganic substances on phase state in real-world aerosol particles was consistent with the results of previous laboratory studies.

In contrast to the Seoul urban area, in Seosan, a significant variation on the RH boundaries for the phase states of the $PM_{2.5}$ was not observed on the polluted *versus* clean days (Figure 3A). This could be resulted from the similar chemical compositions during the entire periods. Figure 3B and S3b show that the abundances of the major chemical species of the $PM_{2.5}$ was insensitive depending on the concentrations. This can be extrapolated to a similar range in the RH boundary of the phase states over the entire period in the coastal-rural area.

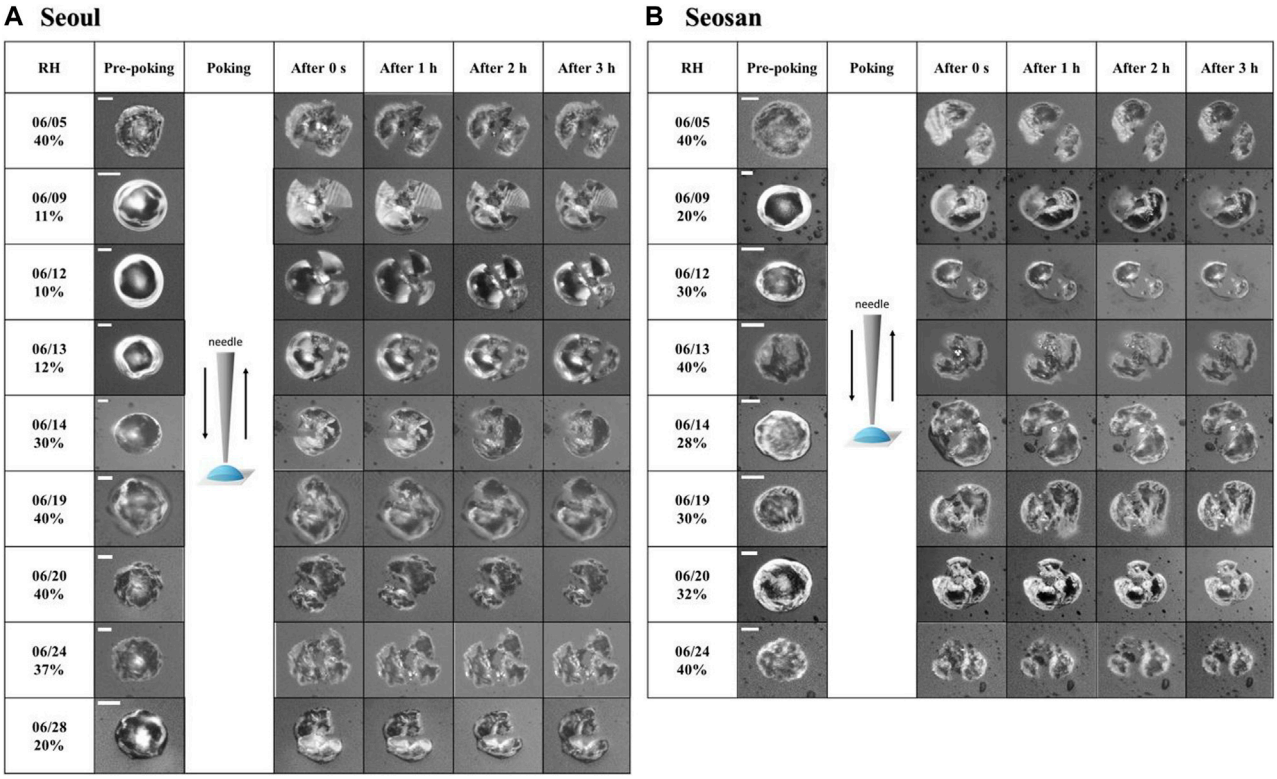

FIGURE 2
Optical images of the poke-and-flow experiment obtained pre-poking, poking, and post-poking of $PM_{2.5}$ droplets in **(A)** Seoul and **(B)** Seosan for cases 1–6. The scale bar represents 10 μm.

3.3 Estimated phase states of $PM_{2.5}$ in urban and coastal-rural areas

The primary impact on the phase state of aerosol particles on RH has been previously studied (Renbaum-Wolff et al., 2013; Song et al., 2015; Reid et al., 2018; Rovelli et al., 2019). From these studies, they explained that aerosol viscosity and phase states are strongly RH-dependent. To estimate the phase state of the bulk of the $PM_{2.5}$, we first related our results to the ambient RH condition of the two sites. Box plots in Figure 3A display the daily ambient RH in Seoul and Seosan. The mean ambient RH during summer was ~70% in Seoul and ~81% in Seosan, with some variations (Figure 3A; Table 1).

Based on the measured phase states of the bulk of the $PM_{2.5}$ (Section 3.2) and mean ambient RH in Seoul (box plot of Figure 3A), $PM_{2.5}$ was estimated in a liquid or semisolid state. The liquid phase state of $PM_{2.5}$ became more dominant as the $PM_{2.5}$ concentration increased when the RH and ammonium nitrate were enhanced. The ambient RH in Seoul (Figure 3A) ranged higher than the deliquescence RH of ammonium nitrate (65.5% RH at 293 K) (Winston and Bates. 1960). This indicates the high ambient RH led to liquefy the $PM_{2.5}$ dominated by ammonium nitrate (Seinfeld and Pandis. 2016). The result is consistent with findings of our recent study of Song et al. (2022) in Seoul during winter where the liquid phase state was dominant on high $PM_{2.5}$ days and a semisolid state was dominant on low $PM_{2.5}$ days. Liu et al. (2017) observed a similar phenomenon where the particle phase state was liquid during heavy haze events in Beijing. Under high RH conditions, rapid chemical reactions can occur between $PM_{2.5}$ and surrounding gas molecules, accelerating the production of high $PM_{2.5}$ mass concentrations.

Most of the $PM_{2.5}$ in Seosan was in a liquid state at the mean ambient RH values, except on June 9, when the RH value was relatively low with an average of ~67% (Figure 3A; Table 1). This coastal-rural area is close to the Yellow Sea (~15 km); therefore, high ambient RH conditions are common. Due to the geographic characteristics of Seosan, $PM_{2.5}$ was commonly existed in a liquid phase state.

In addition to RH, the chemical composition of $PM_{2.5}$ is another important parameter for determining phase states. Several studies have shown that the phase states of aerosol particles were determined by the presence of organic materials, inorganic salts, and their ratios (Rovelli et al., 2019; Richards et al., 2020; Jeong et al., 2022). Using the RH and $PM_{2.5}$ chemical compositions (Supplementary Section S3), the aerosol liquid water content (ALWC) at the two sites were calculated (Figure 3B). As discussed above, a high fraction of inorganic substances in $PM_{2.5}$ was observed at both sites during high $PM_{2.5}$ episodes (Supplementary Figure S3). High inorganic composition and RH could result in abundant liquid water molecules in the $PM_{2.5}$, leading to $PM_{2.5}$ pollution (Supplementary Figure S4). Moreover, a distinct difference in ALWC was observed at the two different sites, with Seosan exhibiting a significantly greater ALWC than Seoul, resulting in a predominantly liquid state of $PM_{2.5}$ in Seosan. To gain more

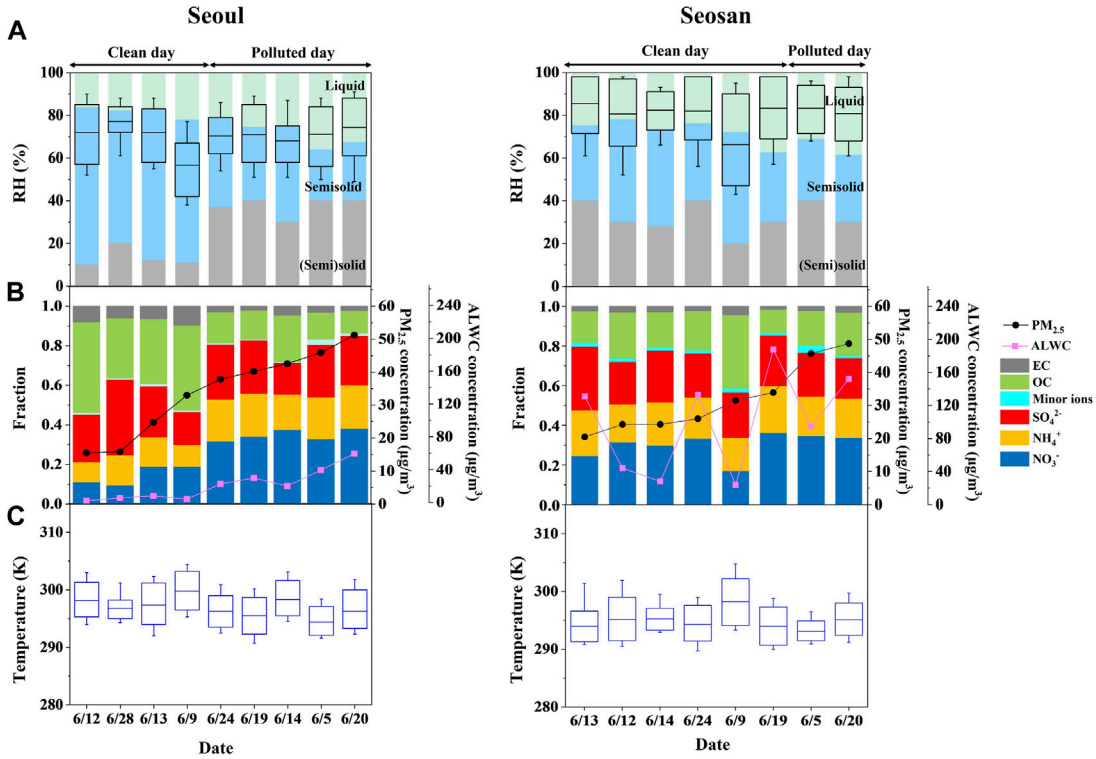

FIGURE 3
Daily average measurement results for $PM_{2.5}$ in Seoul and Seosan on clean ($PM_{2.5}$ < 35 μg/m^3) and polluted ($PM_{2.5}$ ≥ 35 μg/m^3) days in cases 1–6. **(A)** Phase states of the bulk of $PM_{2.5}$ as measured at 293 ± 1 K. Green: liquid; blue: semisolid; and grey: (semi) solid. The box plot indicates daily ambient relative humidity (RH). **(B)** $PM_{2.5}$ mass concentrations, and chemical compositions (minor ions: Cl^-, Na^+, K^+, Mg^{2+}, and Ca^{2+}) and aerosol liquid water content (ALWC). **(C)** Ambient temperature. In the box plot, the box represents the mean, 25th, and 75th percentiles, and the whisker represents the minimum and maximum values. Dates are arranged from low to high $PM_{2.5}$ mass concentrations for cases 1–6.

comprehensive results of the effect of chemical composition on the phase state of ambient aerosol particles, further studies are required with more extensive datasets. In addition, environmental factors such as wind and precipitation could also affect phase variation of $PM_{2.5}$. These parameters should be also considered to explore phase behavior of $PM_{2.5}$.

4 Conclusion and implications

In this study, optical microscopy was combined with the poke-and-flow technique to determine the morphology and phase state of $PM_{2.5}$ at 293 ± 1 K collected in Seoul (urban) and Seosan (coastal-rural) in June 2021. Upon dehydration, the $PM_{2.5}$ droplets from Seoul and Seosan exhibited different morphologies and phases, including single liquid, semisolid, and (semi) solid states. Based on the ambient average RH level and the results obtained from the laboratory experiments at 293 ± 1 K, which is considered similar to ambient temperature, the phase states of bulk $PM_{2.5}$ in the urban and rural areas were estimated. The $PM_{2.5}$ in Seoul was to be in both liquid and semisolid states and results showed that a liquid state was abundant during highly polluted summer days. However, $PM_{2.5}$ was to be present in a liquid state due to the high ALWC, as well as meteorological and geographic characteristics of Seosan. Our results could have several limitations in providing of quantification of viscosity for $PM_{2.5}$ particles, and potential effects of water-insoluble materials on the morphology and phase state. Therefore, to obtain more concrete conclusion for the phase state of $PM_{2.5}$, more experimental dataset and incorporation with different methods are required.

The phase state of aerosol particles can be affected by particle size distribution. Several recent laboratory and modeling studies demonstrated that liquid particles allow the partitioning of gas molecules into the volume of the whole particle with fast reaction/uptake of ambient gas molecules (Shiraiwa et al., 2013; Slade and Knopf. 2014; Berkemeier et al., 2016; Houle et al., 2018). However, for solid particles, gas molecules can only partition onto the surface of the particles. As a result, the phase states of particles can influence particle growth, internal mixing, and particle size distribution (Zaveri et al., 2014; Song et al., 2022). To build on the results from this study, more detailed data is needed to understand the fundamental physical properties of $PM_{2.5}$, and its environmental consequences, which are still largely unknown, and how the physical properties are linked to the chemical compositions that cause $PM_{2.5}$ pollution.

Data availability statement

The original contributions presented in the study are included in the article/Supplementary Material, further inquiries can be directed to the corresponding author.

Author contributions

This study is designed by MS. All of the authors took measurements and analyzed the data. The manuscript was prepared by MS, SG, and DK with contributions from all co-authors. The published version of the manuscript has been read and approved by all authors.

Funding

Fine Particle Research Initiative in East Asia Considering National Differences (FRIEND) Project (NRF-2020M3G1A1114548) and research funds of Jeonbuk National University in 2022.

Acknowledgments

We thank to Sangmin Oh and Junsu Park for helping some filter sampling.

Conflict of interest

The authors declare that the research was conducted in the absence of any commercial or financial relationships that could be construed as a potential conflict of interest.

Publisher's note

All claims expressed in this article are solely those of the authors and do not necessarily represent those of their affiliated organizations, or those of the publisher, the editors and the reviewers. Any product that may be evaluated in this article, or claim that may be made by its manufacturer, is not guaranteed or endorsed by the publisher.

Supplementary material

The Supplementary Material for this article can be found online at: https://www.frontiersin.org/articles/10.3389/fenvs.2023.1142941/full#supplementary-material

References

Bateman, A. P., Gong, Z., Liu, P., Sato, B., Cirino, G., Zhang, Y., et al. (2016). Sub-micrometre particulate matter is primarily in liquid form over Amazon rainforest. *Nat. Geosci.* 9 (1), 34–37. doi:10.1038/ngeo2599

Berkemeier, T., Steimer, S. S., Krieger, U. K., Peter, T., Pöschl, U., Ammann, M., et al. (2016). Ozone uptake on glassy, semi-solid and liquid organic matter and the role of reactive oxygen intermediates in atmospheric aerosol chemistry. *Phys. Chem. Chem. Phys.* 18 (18), 12662–12674. doi:10.1039/C6CP00634E

Bertram, A. K., Martin, S. T., Hanna, S. J., Smith, M. L., Bodsworth, A., Chen, Q., et al. (2011). Predicting the relative humidities of liquid-liquid phase separation, efflorescence, and deliquescence of mixed particles of ammonium sulfate, organic material, and water using the organic-to-sulfate mass ratio of the particle and the oxygen-to-carbon elemental ratio of the organic component. *Atmos. Chem. Phys.* 11 (21), 10995–11006. doi:10.5194/acp-11-10995-2011

Bhattarai, G., Lee, J. B., Kim, M. H., Ham, S., So, H. S., Oh, S., et al. (2020). Maternal exposure to fine particulate matter during pregnancy induces progressive senescence of hematopoietic stem cells under preferential impairment of the bone marrow microenvironment and aids development of myeloproliferative disease. *Leukemia* 34 (5), 1481–1484. doi:10.1038/s41375-019-0665-8

Champion, W. M., Rothfuss, N. E., Petters, M. D., and Grieshop, A. P. (2019). Volatility and viscosity are correlated in terpene secondary organic aerosol formed in a flow reactor. *Environ. Sci. Technol. Lett.* 6 (9), 513–519. doi:10.1021/acs.estlett.9b00412

Cheng, Z., Sharma, N., Tseng, K.-P., Kovarik, L., and China, S. (2021). Direct observation and assessment of phase states of ambient and lab-generated sub-micron particles upon humidification. *RSC Adv.* 11 (25), 15264–15272. doi:10.1039/D1RA02530A

Ciobanu, V. G., Marcolli, C., Krieger, U. K., Weers, U., and Peter, T. (2009). Liquid-liquid phase separation in mixed organic/inorganic aerosol particles. *J. Phys. Chem. A* 113 (41), 10966–10978. doi:10.1021/jp905054d

Gaikwad, S., Jeong, R., Kim, D., Lee, K., Jang, K., Kim, C., et al. (2022). Microscopic observation of a liquid-liquid-(semi)solid phase in polluted PM2.5. *Front. Environ. Sci.* 1126. doi:10.3389/fenvs.2022.947924

Grayson, J. W., Zhang, Y., Mutzel, A., Renbaum-Wolff, L., Böge, O., Kamal, S., et al. (2016). Effect of varying experimental conditions on the viscosity of <i>α</i>-pinene derived secondary organic material. *Atmos. Chem. Phys.* 16 (10), 6027–6040. doi:10.5194/acp-16-6027-2016

Ham, S., Babar, Z. B., Lee, J. B., Lim, H.-J., and Song, M. (2019). Liquid–liquid phase separation in secondary organic aerosol particles produced from <i>α</i>-pinene ozonolysis and <i>α</i>-pinene photooxidation with/without ammonia. *Atmos. Chem. Phys.* 19 (14), 9321–9331. doi:10.5194/acp-19-9321-2019

Houle, F. A., Wiegel, A. A., and Wilson, K. R. (2018). Changes in reactivity as chemistry becomes confined to an interface. The case of free radical oxidation of C30H62 alkane by OH. *J. Phys. Chem. Lett.* 9 (5), 1053–1057. doi:10.1021/acs.jpclett.8b00172

Huang, H., Ho, K. F., Lee, S. C., Tsang, P. K., Ho, S. S. H., Zou, C. W., et al. (2012). Characteristics of carbonaceous aerosol in PM2.5: Pearl delta river region, China. *Atmos. Res.* 104, 227–236. doi:10.1016/j.atmosres.2011.10.016

Jeong, R., Lilek, J., Zuend, A., Xu, R., Chan, M. N., Kim, D., et al. (2022). Viscosity and physical state of sucrose mixed with ammonium sulfate droplets. *Atmos. Chem. Phys. Discuss.* 1-21, 8805–8817. doi:10.5194/acp-22-8805-2022

Jimenez, J. L., Canagaratna, M., Donahue, N., Prevot, A., Zhang, Q., Kroll, J. H., et al. (2009). Evolution of organic aerosols in the atmosphere. *Science* 326 (5959), 1525–1529. doi:10.1126/science.1180353

Ju, S., Yu, G. H., Park, S., Lee, J., Lee, S., Jee, J., et al. (2020). Pollution characteristics of PM2.5 measured during fall at a seosan site in chungcheong province. *J. Korean Soc. Atmos.* 36 (3), 329–345. doi:10.5572/KOSAE.2020.36.3.329

Kim, N. K., Kim, Y. P., Ghim, Y. S., Song, M., Kim, C. H., Jang, K. S., et al. (2022). Spatial distribution of PM2.5 chemical components during winter at five sites in Northeast Asia: High temporal resolution measurement study. *Atmos. Environ.* 290, 119359. doi:10.1016/j.atmosenv.2022.119359

Kim, Y., Sartelet, K., and Couvidat, F. (2019). Modeling the effect of non-ideality, dynamic mass transfer and viscosity on SOA formation in a 3-D air quality model. *Atmos. Chem. Phys.* 19 (2), 1241–1261. doi:10.5194/acp-19-1241-2019

Knopf, D. A., Alpert, P. A., and Wang, B. (2018). The role of organic aerosol in atmospheric ice nucleation: A review. *ACS Earth Space Chem.* 2 (3), 168–202. doi:10.1021/acsearthspacechem.7b00120

Koop, T., Bookhold, J., Shiraiwa, M., and Poschl, U. (2011). Glass transition and phase state of organic compounds: Dependency on molecular properties and implications for secondary organic aerosols in the atmosphere. *Phys. Chem. Chem. Phys.* 13 (43), 19238–19255. doi:10.1039/C1CP22617G

Krieger, U. K., Marcolli, C., and Reid, J. P. (2012). Exploring the complexity of aerosol particle properties and processes using single particle techniques. *Chem. Soc. Rev.* 41 (19), 6631–6662. doi:10.1039/C2CS35082C

Kwamena, N. O., Buajarern, J., and Reid, J. P. (2010). Equilibrium morphology of mixed organic/inorganic/aqueous aerosol droplets: Investigating the effect of relative humidity and surfactants. *J. Phys. Chem. A* 114 (18), 5787–5795. doi:10.1021/jp1003648

Lam, H. K., Xu, R., Choczynski, J., Davies, J. F., Ham, D., Song, M., et al. (2021). Effects of liquid–liquid phase separation and relative humidity on the heterogeneous OH oxidation of inorganic–organic aerosols: Insights from methylglutaric acid and ammonium sulfate particles. *Atmos. Chem. Phys.* 21 (3), 2053–2066. doi:10.5194/acp-21-2053-2021

Li, Z., Smith, K. A., and Cappa, C. D. (2018). Influence of relative humidity on the heterogeneous oxidation of secondary organic aerosol. *Atmos. Chem. Phys.* 18 (19), 14585–14608. doi:10.5194/acp-18-14585-2018

Liu, Y., Li, H., Cui, S., Nie, D., Chen, Y., and Ge, X. (2021a). Chemical characteristics and sources of water-soluble organic nitrogen species in PM2. 5 in nanjing, China. *Atmosphere* 12 (5), 574. doi:10.3390/atmos12050574

Liu, Y., Meng, X., Wu, Z., Huang, D., Wang, H., Chen, J., et al. (2021b). The particle phase state during the biomass burning events. *Sci. Total Environ.* 792, 148035. doi:10.1016/j.scitotenv.2021.148035

Liu, Y., Wu, Z., Wang, Y., Xiao, Y., Gu, F., Zheng, J., et al. (2017). Submicrometer particles are in the liquid state during heavy haze episodes in the urban atmosphere of beijing, China. *Environ. Sci. Technol. Lett.* 4 (10), 427–432. doi:10.1021/acs.estlett.7b00352

Masson-Delmotte, V., Zhai, P., Connors, S. L., Péan, C., and Berger, S. (2021). *IPCC, 2021: Climate change 2021: The physical science basis*. Contribution of Working Group I to the Sixth Assessment Report of the Intergovernmental Panel on Climate Change. United Kingdom and New York, NY, USA: Cambridge University Press, Cambridge, 3–32. doi:10.1017/9781009157896.001

Mikhailov, E. F., Pöhlker, M. L., Reinmuth-Selzle, K., Vlasenko, S. S., Krüger, O. O., Fröhlich-Nowoisky, J., et al. (2021). Water uptake of subpollen aerosol particles: Hygroscopic growth, cloud condensation nuclei activation, and liquid–liquid phase separation. *Atmos. Chem. Phys.* 21 (9), 6999–7022. doi:10.5194/acp-21-6999-2021

Ministry of Environment (2021). *2021: Annual report of air quality in Korea, 2020*, 405.

Petters, S. S., Kreidenweis, S. M., Grieshop, A. P., Ziemann, P. J., and Petters, M. D. (2019). Temperature-and humidity-dependent phase states of secondary organic aerosols. *Geophys. Res. Lett.* 46 (2), 1005–1013. doi:10.1029/2018GL080563

Pöhlker, C., Wiedemann, K. T., Sinha, B., Shiraiwa, M., Gunthe, S. S., Smith, M., et al. (2012). Biogenic potassium salt particles as seeds for secondary organic aerosol in the Amazon. *Science* 337 (6098), 1075–1078. doi:10.1126/science.1223264

Reid, J. P., Bertram, A. K., Topping, D. O., Laskin, A., Martin, S. T., Petters, M. D., et al. (2018). The viscosity of atmospherically relevant organic particles. *Nat. Commun.* 9 (1), 956. doi:10.1038/s41467-018-03027-z

Reid, J. P., Dennis-Smither, B. J., Kwamena, N. O. A., Miles, R. E., Hanford, K. L., and Homer, C. J. (2011). The morphology of aerosol particles consisting of hydrophobic and hydrophilic phases: Hydrocarbons, alcohols and fatty acids as the hydrophobic component. *Phys. Chem. Chem. Phys.* 13 (34), 15559–15572. doi:10.1039/C1CP21510H

Renbaum-Wolff, L., Grayson, J. W., Bateman, A. P., Kuwata, M., Sellier, M., Murray, B. J., et al. (2013). Viscosity of alpha-pinene secondary organic material and implications for particle growth and reactivity. *Proc. Natl. Acad. Sci. U. S. A.* 110 (20), 8014–8019. doi:10.1073/pnas.1219548110

Richards, D. S., Trobaugh, K. L., Hajek-Herrera, J., Price, C. L., Sheldon, C. S., Davies, J. F., et al. (2020). Ion-molecule interactions enable unexpected phase transitions in organic-inorganic aerosol. *Sci. Adv.* 6 (47), eabb5643. doi:10.1126/sciadv.abb5643

Riemer, N., Ault, A., West, M., Craig, R., and Curtis, J. (2019). Aerosol mixing state: Measurements, modeling, and impacts. *Rev. Geophys* 57 (2), 187–249. doi:10.1029/2018RG000615

Rothfuss, N. E., and Petters, M. D. (2017). Influence of functional groups on the viscosity of organic aerosol. *Environ. Sci. Technol.* 51 (1), 271–279. doi:10.1021/acs.est.6b04478

Rovelli, G., Song, Y.-C., Maclean, A. M., Topping, D. O., Bertram, A. K., and Reid, J. P. (2019). Comparison of approaches for measuring and predicting the viscosity of ternary component aerosol particles. *Anal. Chem.* 91 (8), 5074–5082. doi:10.1021/acs.analchem.8b05353

Seinfeld, J. H., and Pandis, S. N. (2016). *Atompspheric chemistry and physics from air pollution to climate change*. John Wiley & Sons.

Shiraiwa, M., Yee, L. D., Schilling, K. A., Loza, C. L., Craven, J. S., Zuend, A., et al. (2013). Size distribution dynamics reveal particle-phase chemistry in organic aerosol formation. *Proc. Natl. Acad. Sci.* 110 (29), 11746–11750. doi:10.1073/pnas.1307501110

Slade, J. H., and Knopf, D. A. (2014). Multiphase OH oxidation kinetics of organic aerosol: The role of particle phase state and relative humidity. *Geophys. Res. Lett.* 41 (14), 5297–5306. doi:10.1002/2014GL060582

Song, M., Jeong, R., Kim, D., Qiu, Y., Meng, X., Wu, Z., et al. (2022). Comparison of phase states of PM2.5 over megacities, Seoul and beijing, and their implications on particle size distribution. *Environ. Sci. Technol.* 56 (24), 17581–17590. doi:10.1021/acs.est.2c06377

Song, M., Liu, P. F., Hanna, S. J., Li, Y. J., Martin, S. T., and Bertram, A. K. (2015). Relative humidity-dependent viscosities of isoprene-derived secondary organic material and atmospheric implications for isoprene-dominant forests. *Atmos. Chem. Phys.* 15 (9), 5145–5159. doi:10.5194/acp-15-5145-2015

Song, M., Maclean, A. M., Huang, Y. Z., Smith, N. R., Blair, S. L., Laskin, J., et al. (2019). Liquid-liquid phase separation and viscosity within secondary organic aerosol generated from diesel fuel vapors. *Atmos. Chem. Phys.* 19 (19), 12515–12529. doi:10.5194/acp-19-12515-2019

Song, M., Marcolli, C., Krieger, U. K., Lienhard, D. M., and Peter, T. (2013). Morphologies of mixed organic/inorganic/aqueous aerosol droplets. *Faraday Discuss.* 165, 289–316. doi:10.1039/C3FD00049D

Song, M., Marcolli, C., Krieger, U. K., Zuend, A., and Peter, T. (2012). Liquid-liquid phase separation and morphology of internally mixed dicarboxylic acids/ammonium sulfate/water particles. *Atmos. Chem. Phys.* 12 (5), 2691–2712. doi:10.5194/acp-12-2691-2012

Song, Y. C., Lilek, J., Lee, J. B., Chan, M. N., Wu, Z. J., Zuend, A., et al. (2021). Viscosity and phase state of aerosol particles consisting of sucrose mixed with inorganic salts. *Atmos. Chem. Phys.* 21 (13), 10215–10228. doi:10.5194/acp-21-10215-2021

Song, Y., Huang, B., He, Q., Chen, B., Wei, J., and Mahmood, R. (2019). Dynamic assessment of PM2.5 exposure and health risk using remote sensing and geo-spatial big data. *Environ. Pollut.* 253, 288–296. doi:10.1016/j.envpol.2019.06.057

Winston, P. W., and Bates, D. H. (1960). Saturated solutions for the control of humidity in biological research. *Ecology* 41 (1), 232–237. doi:10.2307/1931961

You, Y., Renbaum-Wolff, L., Carreras-Sospedra, M., Hanna, S. J., Hiranuma, N., Kamal, S., et al. (2012). Images reveal that atmospheric particles can undergo liquid-liquid phase separations. *Proc. Natl. Acad. Sci. U. S. A.* 109 (33), 13188–13193. doi:10.1073/pnas.1206414109

Zaveri, R. A., Easter, R. C., Shilling, J. E., and Seinfeld, J. H. (2014). Modeling kinetic partitioning of secondary organic aerosol and size distribution dynamics: Representing effects of volatility, phase state, and particle-phase reaction. *Atmos. Chem. Phys.* 14 (10), 5153–5181. doi:10.5194/acp-14-5153-2014

Zaveri, R. A., Shilling, J. E., Zelenyuk, A., Liu, J., Bell, D. M., D'Ambro, E. L., et al. (2018). Growth kinetics and size distribution dynamics of viscous secondary organic aerosol. *Environ. Sci. Technol.* 52 (3), 1191–1199. doi:10.1021/acs.est.7b04623

Zhang, Q., Jimenez, Z. L., Canagaratna, M. R., Ulbrich, I. M., Ng, N. L., Worsnop, D. R., et al. (2011). Understanding atmospheric organic aerosols via factor analysis of aerosol mass spectrometry: A review. *Ananl. Bioanal. Chem.* 401, 3045–3067. doi:10.1007/s00216-011-5355-y

Zuend, A., and Seinfeld, J. H. (2012). Modeling the gas-particle partitioning of secondary organic aerosol: The importance of liquid-liquid phase separation. *Atmos. Chem. Phys.* 12 (9), 3857–3882. doi:10.5194/acp-12-3857-2012